Size Determination of Gold Clusters by Polyacrylamide Gel Electrophoresis in a Large Cluster Region

ARTICLE *in* THE JOURNAL OF PHYSICAL CHEMISTRY C · AUGUST 2009

Impact Factor: 4.77 · DOI: 10.1021/jp808967p

6 AUTHORS, INCLUDING:

Keisaku Kimura
Hosei University
186 PUBLICATIONS **3,732** CITATIONS

SEE PROFILE

Yuichi Negishi
Tokyo University of Science
89 PUBLICATIONS **4,452** CITATIONS

SEE PROFILE

ARTICLES

Size Determination of Gold Clusters by Polyacrylamide Gel Electrophoresis in a Large Cluster Region

Keisaku Kimura,*,† Nobuyuki Sugimoto,† Seiichi Sato,† Hiroshi Yao,† Yuichi Negishi,‡,§ and Tatsuya Tsukuda‡,||

Department of Material Science, Graduate School of Science, University of Hyogo, Koto 3-2-1, Kamigori-cho, Ako-gun, Hyogo 678-1297, Japan, and Research Center for Molecular-Scale Nanoscience, Institute for Molecular Science, Myodaiji, Okazaki 444-8585, Japan

Received: October 10, 2008; Revised Manuscript Received: June 26, 2009

Polyacrylamide gel electrophoresis (PAGE) is used to separate the component of the glutathione protected gold clusters up to Au_{160} core size and compare the size with the mobility data from PAGE. Both electrospray mass spectrometry and transmission electron microscopy were systematically applied to analyze Au−glutathione clusters thus isolated. We have found a linear relationship between the mobility of the gold cluster compounds to the logarithm of the number of gold atoms of the core. Better fitting to the logarithm of the number of thiolate molecules adsorbed on the gold core was found and was expressed by a simple equation that bears conformation of ligand and charge density of clusters. Hence the mobility of the metallic clusters was correlated to the component of the ligand of the cluster.

Introduction

Gold clusters and nanoparticles are of current concern due to their wide applications in catalysis, nanobiotechnology, biosensing and lithography as well as importance in basic science such as the Kubo effect. The physicochemical properties of these materials are highly sensitive to their size and shape so that isolation of the particles as a function of size and determination of their size as well as shape is the first step in the characterization process. Polyacrylamide gel electrophoresis (PAGE) is a simple and powerful tool for isolation and determination of the molecular weights of proteins[1a] and DNA,[1b] and the methodology is well established in biochemistry. There are many standard polypeptides known for the molecular weight scale such as myosin, RNA polymerase, phosphorylase, bovine serum albumin, catalase, ovalbumin, carbonic anhydrase horse heart myoglobin, lysozyme and cytochrome *c*, etc.[2] The R_f values derived from mobility of standard proteins listed above are frequently used to determine the molecular weight of unknown proteins. The size of catalase reaches 5 nm indicating that we can evaluate a large size up to 5 nm solely from the PAGE method. Regardless of recent developments in gold cluster and nanoparticle science, little is known on the determination of the cluster size or molecular weight of the clusters by PAGE method. One example is the isoelectric focusing in a polyacrylamide pH gradient gel, which was used to sharpen the size distribution of gold particles.[3] PAGE was also used to estimate the conformation of oligonucleotides attached to the surface of gold nanocrystals of 10 nm in size.[4] However, no trial was reported to determine the size of particles solely from the PAGE method.

Well-known standard methods for the size determination of metal clusters are transmission electron microscopy (TEM) and mass spectrometry; both require sophisticated instrumentation or a special technique in vacuum. The former is often applied to large clusters whose core sizes are larger than 2 nm,[5] and the latter is used when the sizes of clusters are less than 1.5 nm.[6] The typical PAGE technique available for the determination of the mass of proteins and nucleic acids utilizes the linear relationship between the mobility of unfolded polypeptide and the molecular weight of the peptide chain on the homogeneous gel constituent. Sometimes, linear gradient gel mixtures can be also used to determine the molecular weight to cover a broad mass range. These techniques are effective for compounds with homogeneous constituents such as unfolded polypeptide, denatured proteins or enzymes. We are not aware of the use of PAGE techniques in the literature for determining the structural parameters of metallic nanoparticles, which comprise central hard cores surrounded by soft organic ligands. In recent reports, we applied the small-angle X-ray scattering (SAXS) technique to determine the size of gold and silver nanoclusters[7−9] and found a linear relationship between the mobility of clusters separated by PAGE and the size by SAXS.[9] However, the SAXS technique is only effective for the metallic core and gives no information on the protecting organic moiety.

Glutathione (reduced form, GSH) is a ubiquitous tripeptide found in biological systems. Gold clusters protected by self-assembled monolayers of GSH were isolated to single species,[10−12] and their composition was examined systematically up to $Au_{39}(SG)_{24}$ by mass spectrometric methods.[13,14]

* Corresponding author. E-mail: kimura@sci.u-hyogo.ac.jp. Phone: +81-791-58-0159. Fax: +81-791-58-0161.
† University of Hyogo.
‡ Institute for Molecular Science.
§ Current address: Department of Applied Chemistry, Faculty of Science, Tokyo University of Science, Kagurazaka, Shinjuku-ku, Tokyo 162-8601, Japan.
|| Current address: Section of Catalytic Assemblies, Catalysis Research Center, Hokkaido University, Sapporo 001-0021, Japan.

10.1021/jp808967p CCC: $40.75
Published on Web 07/17/2009

Hence, $Au_n(SG)_m$ can be regarded as a model cluster compound to other type of water-soluble gold clusters. In the present report, we aim to encompass the size regime from magic numbered small cluster to a large cluster whose size extends to 1.8 nm and to express the molecular weight of the cluster by a simple relation to the R_f value. We also aim to determine the limit of the PAGE technique to separate a large core−shell type cluster. We report how the size and structure of water-soluble gold clusters reflect to the polyacrylamide gel electrophoretic pattern and to the mobility of each cluster beyond $Au_{39}(SG)_{24}$. The electrospray ionization (ESI) mass spectrometry was engaged to correlate the mass and component of isolated clusters to the relative mobility (R_f value) of the clusters in the small size region, and TEM was used in the large size region. We have observed distinct variation in the slope of the mobility plot as a function of gold core size at around Au_{40} against our expectation. We have discussed a possible cause of this finding.

Experimental Section

All starting materials were used as purchased. The synthesis of surface modified gold clusters was followed by an established method,[12,15] which was slightly modified appropriate to large cluster formation. All the synthetic processes were conducted under ice−water temperature, dark and anaerobic conditions. The methanol solution (100 mL) of $HAuCl_4$ (0.5 mM) was added to 0.1 mmol of GSH in Erlenmeyer flask (500 mL) and kept at 0 °C under Ar gas flow. The aqueous solution of $NaBH_4$ (0.2 M, 25 mL), cooled at 0 °C, was sprayed within 20 s into the mixture under vigorous stirring. The mixture was kept with mild stirring for another 1.5 h under an Ar flow. After keeping overnight at quiet condition, the resulting precipitate was collected and washed twice with a water/methanol mixture (1:9) under sonication through centrifugal separation. The washed samples were condensed with a rotary evaporator and dried in vacuum to obtain a dark brownish sample powder, yielding ∼150 mg.

Among the PAGE methods applied to the separation of gold−thiolate clusters, a technique using homogeneous gel concentration is found in the literature.[7−14] This method is effective for the smaller size region such as Au_n ($n < 60$). Thus we have engaged in homogeneous gel separation in ESI analysis because of maintaining consistency with the previous mass determination.[14] Gel-electrophoresis-unit with 2 mm thickness was used to process the PAGE method. As the condition of a homogeneous gel used for ESI mass measurement, 18% and 3% total concentration (acrylamide/bis (acrylamide) = 95:5 by weight) were used for separating and stacking gel, respectively. The eluting buffer consisted of 192 mM glycine and 25 mM tris(hydroxymethylamine). The as-prepared sample powders of 12 mg were dissolved in a 1 mL, 30% sucrose/Tris-HCl buffer solution (pH = 6.8, the same pH for concentration gel) and subjected to gel electrophoresis (pH = 8.8) for about 5 h at ice/water temperature to avoid thermal decomposition. The initial applied field was 150 V, 50 mA. After electrophoresis, each fraction of the gel band was cut out and stored at −80 °C for further treatment. At least five accumulations of the fractions were needed in order to conduct ESI measurement. The gel fractions stocked in a refrigerator were crushed in 10 mL of distilled water and kept at 2 °C for 2 h. The large gel lumps in the solution were filtrated by a 0.2 μm polyvinylidene fluoride filter (MILLEX-GV PVDF). To the filtrate, 1 mL of acetic acid (2%) was added and concentrated to around 0.2 mL. The AuSG clusters were precipitated by addition of 1 mL of methanol and subsequent centrifugation (14000 rpm, 5 min). Addition of methanol and centrifugation process was repeated three times in order to wash the clusters completely. To the precipitates was added 0.6 mL of distilled water followed by further addition of 10 mL of distilled water, and the resultant solution was centrifuged with a 30 kDa polyethersulfone filter (VIVASPIN 20 30000 MWCO PES) to remove large gel fraction three times followed by a 5 kDa polyethersulfone filter (VIVASPIN 20 5000 MWCO PES) to separate small impurities under 4 atmospheric nitrogen gas pressure. The supernatant solution containing AuSG clusters was collected and redissolved again into 10 mL of distilled water. The filtration and centrifugation processes were repeated three more times. Finally, the effluent was lyophilized and a powder sample was gained for ESI mass spectrometry.

While homogeneous gel separation, which is effective for a smaller size cluster, was used in ESI mass analysis in ref 14, we have to cover a wide size range from several tens to hundreds of gold atoms in a large cluster size region in this study. It is difficult to separate each fraction from densely packed band in the homogeneous gel condition so that we engaged in a linear gradient gel condition to isolate each band on one gel sheet. In the latter case, the total acrylamide concentration at the top part is set to 16% (% C = 5) and that of the bottom part is 26% (% C = 5). For the gradient gel operation with 340 min electrophoresis, the gel containing each fraction was cut out, ground and dipped in 4 mL of ice-cooled distilled water for 2 h. Subsequently, the mixture was centrifuged at 7000 rpm for 5 min, followed by filtering using 0.1 μm pores (Ultrafree-MC PVDF) to remove the gel lumps suspended in the solution. This solution was used for the optical measurement. For the TEM observation, the resultant solution after filtration was mixed with 1.0 mL of tetraoctylammonium bromide toluene solution (18.3 μM). By shaking the solution, the dark brown species dissolved in an aqueous phase was quickly transferred into the toluene layer. This method was applied to the sample for TEM, UV−vis optical spectroscopy and electrophoretic mobility measurements. Other conditions were almost the same as for the homogeneous gel except the gel concentration of 18% (30% in ref 14). The relative band sequence does not change between homogeneous and gradient gels. Reproducibility was very good when engaging in homogeneous gel preparation. While in linear gradient gel, the reproducibility is less such as the inclination of the linear line in Figure 4 is slightly changed but the crossing point unchanged. As discussed by Morris and Morris,[2a] the use of discontinuous electrolyte systems and gradient of polymer linkage led to a potential gradient that may induce inaccurate migration through the gel. This is one reason for the lesser reproducibility in the present system than homogeneous system. Each fraction is designated as **1**, **2**, **3** and so forth in the order of mobility.

ESI mass spectra of the fractionated samples were measured by using a homemade apparatus described elsewhere[12,14] (Supporting Information, SI1). TEM measurements were done using a HITACHI H-8100 transmission electron microscope operating at 200 kV. For TEM examination, several drops of the sample solution were casted on a holey carbon coated copper grid and the solvent was evaporated under ambient conditions.

Results and Discussion

It is a common strategy in PAGE technique that the mobility of peptides is correlated with their molecular weight or size.

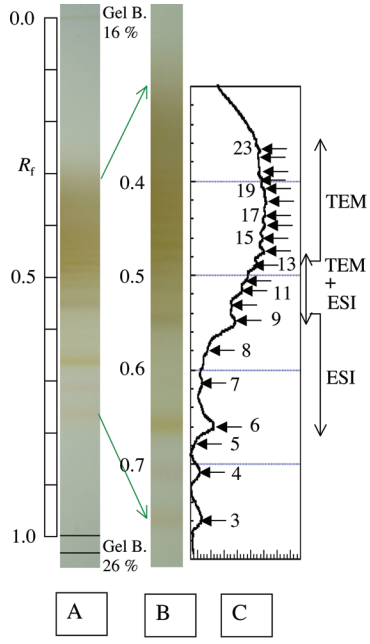

Figure 1. PAGE pattern and numbering of the fraction bands. Panel A shows a whole PAGE pattern after 340 min operation from top of resolving gel of 16% T to the bottom gel boundary (gel B) of 26% T. The second line at the bottom of the gel stands for the position of flowing buffer head which is the position of $R_f = 1$. Note that the initial concentrated sample band around 0.2 mm thickness spreads on the region from $R_f = 0.85$ to 0.25. Panel B is an expansion of the central part of A. Panel C shows the digitized data of the concentration of the band in panel B in which arrows point the precise position of each band.

Hence in the present case, we examine the relation of the position of fraction band to the size of clusters. Figure 1 shows the PAGE pattern and the band position analysis of the expanded region with relative mobility R_f, which is defined by the ratio of the distance migrated by cluster to distance migrated by light molecules. Figure 1A stands for the photograph of gel sheet including resolving gel boundary position and effluent head just after 340 min electrophoresis operation. Panel B is an expanded scale of the middle part of A. Panel C presents a computer manipulation of the contrast of image B, which resolves many bands in the crowded area. From peak position of each band, accurate R_f values could be determined. We could index until **23** or more and cut out the fraction for TEM and ESI measurements. A smaller fraction less than **13** was used for ESI and larger fraction than **9** for TEM observations. To guarantee the accuracy of TEM size determination, we have checked two fractions, **9** and **13**, by both ESI and TEM (see Figure S2A−C in the Supporting Information for the TEM images and their size histograms).

Figure 2 stands for the ESI spectra of AuSG in the mass region from m/z 1500 to 4000. In the present lot, fraction **9** contains mainly the $Au_{38}(SG)_{24}$ (hereafter we have labeled as (38, 24)) component mixed with minor species of (39, 24) which shows small peaks at slightly higher mass side against our earlier report,[14] where (39, 24) is the majority. This is not a surprising fact accounting the kinetic stabilization process,[13] that is sensitive to a difference in the preparation conditions. Fraction **11** consists of (42, 24), (44, 24) and (45, 25), and **13** comprises (54, 28), (56, 29), (58, 29), and (62, 30) (not labeled in the figure) components, respectively. Due to resolution restriction, it is difficult to distinguish the mass position of $(n - 3, m + 2)$ or $(n + 3, m - 2)$ from (n, m), which induces uncertainty in mass

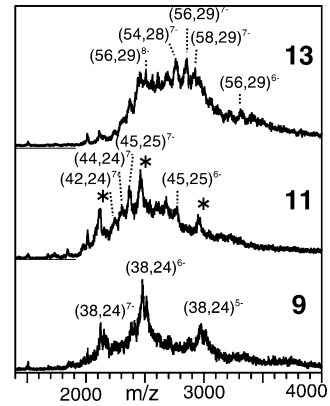

Figure 2. Negative-ion electrospray ionization mass spectra of AuSG clusters in the range 1500−4000 m/z. The mass peaks are assigned to $Au_n(SG)_m^{p-}$ and denoted as $(n, m)^{p-}$. Bold figures refer to fraction numbers in the PAGE band. Mass peaks marked by asterisks in fraction **11** are species from adjacent fractions, (38, 24) or (39, 23).

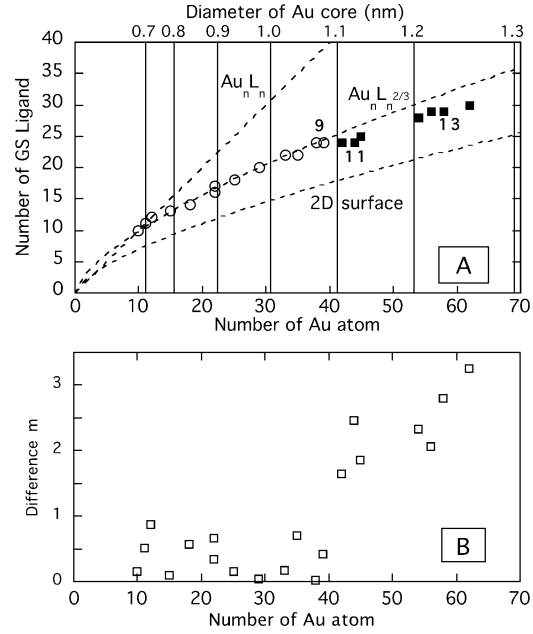

Figure 3. The relation of (n, m) in $Au_n(SG)_m$ determined by ESI mass analysis. Au_nL_n (L = SG) stands for the case in which all Au atoms are exposed to surface. When the particle has compact morphology such as a sphere, we have $m \propto n^{2/3}$ relation. $Au_nL_{n^{2/3}}$ is a fitting curve assuming a spherical shape and packing density 0.15 nm^2. The 2D surface is a curve with bulk packing density 0.21 nm^2. Panel B is a difference of observed m from calculated value by eq 2 as a function of n.

determination solely from ESI of single species. The asterisks in **11** are species from adjacent fractions. These additional structural assignments can be used to correlate the gold to ligand ratio in the cluster, which may reflect the development of structure arising from cluster growth process. Fraction **13** is almost the maximum mass limit to be precisely determined by our mass spectrometer. Beyond this fraction, we have to apply the TEM method. Figure 3 summarizes the chemical composition of the gold cluster by the present data (filled squares) together with the previous one (open circles).[14] In Figure 3A, the linear line stands for 1:1 gold to thiolate ratio, typical case for all Au atoms exposed to GSH molecules which seems to hold for the first three clusters with $n = 10$, 11, and 12. However this ratio does not smoothly connect to bulk structure. In order to correlate the number of gold to that of thiolate, we must examine the structure of Au−SG

clusters. Recent report of crystal structure on $Au_{25}(SR)_{18}$[16] revealed that a central Au_{13} core is surrounded by three $Au_2(SR)_3$ rings and on $Au_{102}(SR)_{44}$[17,18] showing that the Au_{79} core is covered with mixtures of $Au(SR)_2$ and $Au_2(SR)_3$ ring. Theory on $Au_{38}(SR)_{24}$ predicts that $Au(SR)_2$ and $Au_2(SR)_3$ rings cover the Au core.[19] Interestingly, the S to Au ratio gradually approaches the typical value for surface Au:SR = 2:1 when the underlying surface gold atoms in these structures are taken into account. Although the surface structures of these reports are not compatible with the so-called hollow site surface model, we have adopted the model to the calculation for simplicity. Since TEM gives core diameter of clusters, one must derive the total number of gold atoms n and the number of ligand molecules m solely from core diameter D to compare with that by ESI mass data. The diameter of particles can be converted to n with the equation

$$n = 31D^3 \quad (1)$$

where D is in nm, assuming spherical shape and the bulk gold density. The structural modeling on the bulk gold surface concludes Au:SR = 2:1 (as a reference value in the bulk crystallographic data, 0.144 nm^2 per two Au atoms on (111) and 0.166 nm^2 per two Au atoms on (100) surfaces, respectively). That is, the highest occupancy area σ by surface thiolate is 0.15 nm^2.[20,22] From elemental analysis of the small gold particles with 1.2 nm in diameter, it was found that[20,21] one thiolate molecule was bound to 1.84 gold atoms giving occupancy area 0.155 nm^2, consistent with that by structural consideration. We adopted this value as the packing density and using bulk gold density to give the relation of m to n as in the equation

$$m = \frac{\pi D^2}{\sigma} = \frac{\pi}{0.15}\left(\frac{n}{31}\right)^{2/3} = 2.12n^{2/3} \quad (2)$$

As seen in Figure 3A, it is surprising that there is less deviation from the curve by eq 2 which was derived by densely packing approximation, equivalent to the so-called hollow site model or a bidendate ligation, even in the low mass region from Au_{15} to Au_{39}, whereas appreciable deviation was found in the high mass region, against the anticipation that eq 2 should fit well in the high mass region. The observed points seem to deviate from the calculated line over Au_{40}. The plot of the difference of observed m from eq 2 as a function of n clearly shows this deviation and is shown in Figure 3B. It is obvious that the observed m deviates markedly from the calculation for large n value. The deviation is apparent at around $n = 40$. If we assume the occupancy area being 0.163 nm^2, best fit can be attained for **11** and **13**. It is worthy to note that 0.21 nm^2 was reported on the gold plate.[23] Hence, a high occupancy area is not compatible with a gold plate (two-dimensional plane). The overcrowding of adsorbed ligands can be solved for small particles where the staple conformation was suggested.[16] Hence, we expect a structural change in the cluster conformation around this region, where gold to thiolate number ratio has changed. In Table 1, we summarize the size of a cluster D, n and m for each fraction from **2** to **23** using eqs 1 and 2. Before entering into a detailed discussion concerning this deviation, we should examine mobility of the cluster as a function of molecular composition.

TABLE 1: Comparison of the Size of Particle Diameter D with n and m for Fraction Number[a]

fraction	D/nm	n	m
2	0.78	15	13
3	0.83	18	14
4	0.88	22	16
5	0.88	22	17
6	0.92	25	18
7	0.97	29	20
8	1.01	33	22
9	1.03	38	24
9′	1.06	39	24
11	1.12	45	25
13	1.24	56	29
15	1.35	76	36
17	1.44	93	41
19	1.55	115	48
23	1.72	158	59

[a] From **2** to **9**, D was derived from eq 1. From **15** to **23**, n and m were derived from eqs 1 and 2. For parameters for fractions **9**, **9′**, **11** and **13**, both ESI and TEM data were used.

Simple zone electrophoresis in a bulk solution gives the relation of mobility μ to the size of a particle r and the charge Q as

$$\mu = \frac{Q}{6\pi\eta r} \quad (3)$$

where η is viscosity of solvent. It is clear that the mobility is a function of the size of a particle and charge or charge density. This relation can be converted into the Smoluchowski equation using ζ-potential and a dielectric constant of the solvent ε as

$$\mu = \frac{\varepsilon}{\eta}\zeta \quad (4)$$

When ζ-potential is constant, the mobility is also constant irrespective of the size of a particle as found in long chain DNA.[24] This holds for the case of edge contribution being small. Equations 3 and 4 are applicable to free solution. In the PAGE system, it is common knowledge that the migration distance of a species, which is characterized by the R_f value, depends on the size of protein or DNA. Among several formulas that can be compared with the present experiment, the simplest is by eq 5,[25]

$$\mu = \mu_0\left(1 - \frac{\log V}{\log V_{max}}\right) \quad (5)$$

in which μ_0 is given by eq 3 for the smallest molecule that passes through the gel, identically no hindrance to the molecule. V_{max} is the volume of hypothetical large cluster that cannot pass through the gel and a function of the shape of a cluster and the interaction of a ligand of a cluster with gel; the latter seems to be constant in the whole region measured but the former changed as seen in the change of σ appeared around $m = 40$. Beyond $m = 40$, σ is larger than that for $m < 40$. It should be noted that eq 5 is applicable to the cluster group with the same shape, same charge density and the same interaction with the gel.

A plot of R_f values as a function of log n is given in Figure 4A. Error bars on the closed circles reflect the size distribution.

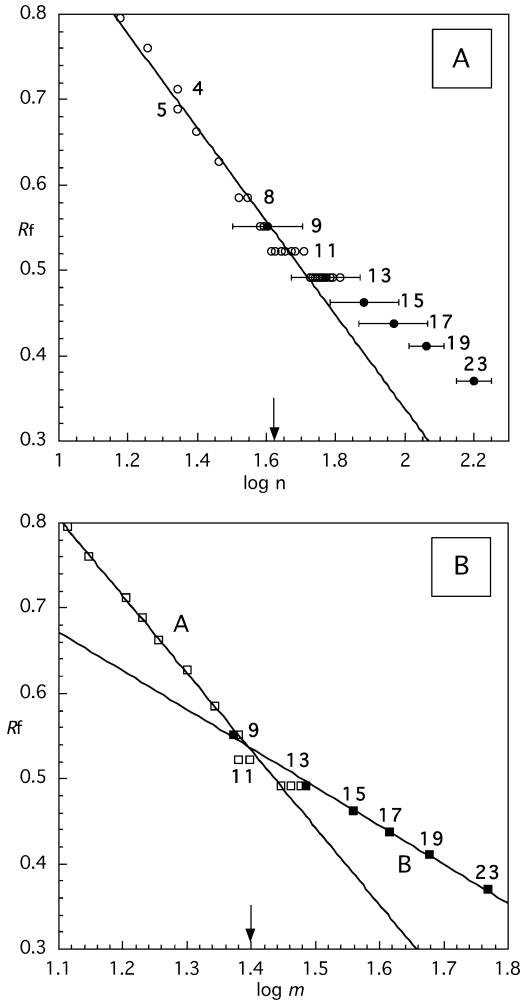

Figure 4. Relationship between relative mobility R_f and logarithm of m and n. Panel A: Open circles are from ESI analysis and bold circles are from TEM observations bearing with size half width. All cluster homologues $Au_{n-3}(SG)_{m+2}$ or $Au_{n+3}(SG)_{m-2}$ for $Au_n(SG)_m$ are also plotted in the same figure. Note that both open and bold circles locate nearly the same position for **9** and **13**. An arrow on the abscissa is $n = 41.7$. Panel B: Open squares are from ESI analysis, and bold squares are from TEM observations. An arrow on the abscissa stands for $m = 25$. In this panel, we omit error bars and AuSG homologues for clarity.

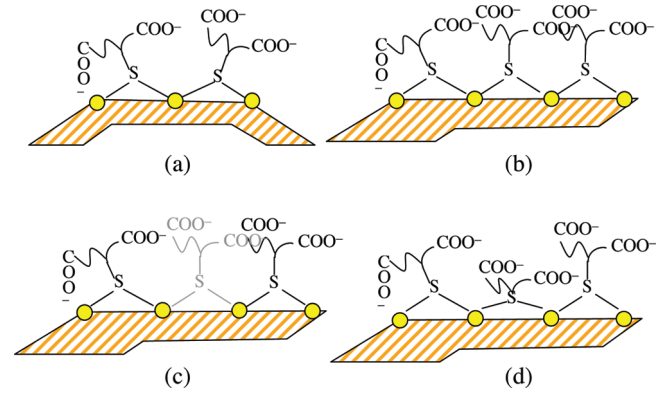

Figure 5. Schematics of conformational change of thiolate induced by a restriction of surface space. Small cluster: (a) There is a lot of free space outside the surface of a small cluster avoiding overcrowding. Large cluster: (b) Thiolate with stand-up geometry conflicts with each other especially at the center part of the surface. To avoid steric hindrance, (c) the position of the center thiolate (gray colored) shifts behind both side holding stand-up geometry. Or, (d) the center thiolate takes lay-flat configuration. Cases (c) and (d) result in increasing occupancy area.

We also draw our attention to possible homologues ($n - 3$, $m + 2$) or ($n + 3$, $m - 2$) in addition to the principal species (n, m) in the same plot. It is clear that there is a kinky point between **9** and **13** at log $n = 1.62$ corresponding to (41, 25) against our expectation of a simple linear relationship between R_f and log n that holds in polypeptide chain. One may question the deviation from linear relationship found in Figure 4A as that originating from the difference in the measurement methods to determine n (such as black circle is TEM and open one is ESI). Fractions **9** ($n = 38$, 39 by ESI) and **13** ($n = 54-62$ by ESI) were checked by TEM (TEM examination supports 40 for **9** and 59 for **13**), and the possibility was ruled out. The deviation is not due to the gel condition, homogeneous or gradient, since the plot in Figure 3, in which the deviation already exists, is from the ESI method using a homogeneous gel. Hence the deviation reflects intrinsic properties of the Au clusters. In that plot, the whole region seems to separate two regions. A linear line with a large slope fits well for smaller than $n = 40$ (corresponding to $m = 25$), and a small slope does well for a larger cluster. The crossing point of two regions located at $n =$ 41 can be compared with the point where a large deviation appears in Figure 3. Much better plots are obtained when we convert n to m using eq 2 as shown in panel B. Here we omit error bars in mass plots for clarity. Overlapping of fractions (**4** and **5**, **8**, **9**) in panel A is isolated or unified giving a better fit. The difference of the slope in both plots of R_f vs log m and log n questions the assumption of occupancy density = 0.15 nm^2 which was used in eq 2. That is, difference in occupancy area might suggest the difference in the orientation or conformation of ligand on the surface of clusters in regions A and B such as standing up (densely packing) or lying flat (loosely packing), or the configuration and composition of capping ligands varies around this region, which may gradually approach to the structure of ligand on bulk surface as cluster size grows. In Figure 5, we present possible diagrams showing how the conformation of thiolate changes depending on the particle size and how it reflects in the occupancy area. For small clusters, large surface curvature enables the ligand to form closest packing without overcrowding (case (a)). However for a large cluster with flat facet, there are many lattice points in which adsorbed thiolates conflict with each other if densely packed (case (b)). To avoid this steric hindrance, there are two typical possibilities. In one case, the position of one thiolate (colored gray) shifts laterally, leading increase of the occupancy area (case (c)). Another configuration is case (d) in which one of the thiolate takes the lying flat configuration, resulting in enhancement of occupancy area.

The variation of the slope as a function of the logarithm of size is against our expectation. We tried to explain this finding within the framework of the standard PAGE theory. Since electrophoresis was performed at around alkaline pH as stated in the Experimental Section, all carboxylic acids are ionized so that mobility is a function of the total number of charged GSH molecules adsorbed on the cluster surface and the size of clusters. Hence the number of GSH molecules affects both surface charge and the size of clusters, whereas gold core works solely on the size of the clusters. That is, metal core makes a marginal contribution to the gel separation. This is why a good fitting is obtained for the R_f vs log m plot (panel B of Figure

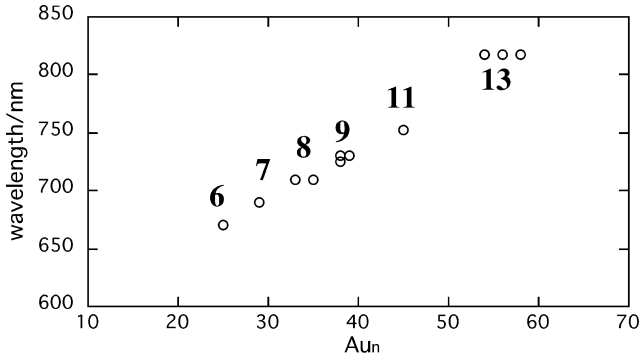

Figure 6. A plot of the first absorption peak of each component in the large cluster region as a function of number of Au atoms.

4). More quantitatively, V_{max} in eq 5 can be related to σ through eq 2 for given m.

$$V_{max} = \frac{\sqrt{\pi}}{6}(m_{max}\sigma)^{3/2} \quad (6)$$

where m_{max} is the number of ligands of the particle that cannot pass through the gel. The slope of the plot in Figure 4B is given by $\mu_0/(\log V_{max})$, leading to $1/\sigma^{3/2}$ dependence, that is to say, the slope is smaller for large σ at given m. Introducing σ-values for both small and large m region, we have a theoretical slope ratio $(0.15/0.163)^{3/2} = 0.88$ whereas the observed one is 0.5. Furthermore, variation of σ might induce change of the surface charge density. However, no apparent expression is incorporated in eq 5 within the frame of existing theory. If we assume that μ_0 is the mobility of a hypothetical small molecule that has the same charge density as that of the clusters in question, μ_0 in eq 5 can be converted to $\mu_0(\sigma_0/\sigma)$. Hence overall, the relative slope is given by the ratio of $(\sigma_0/\sigma)^{5/2} = 0.81$, not in quantitative agreement with 0.5. However, qualitative behavior is explained within the current knowledge.

In conclusion, the main factor of separation is ascribable to the organic moiety of the cluster. Replacing thiolate side chain to a bit bulkier structure induced upward shift, hence small mobility, on the elution pattern of PAGE as found in the literature.[13,14] This finding is consistent with the general tendency of PAGE separation such as the larger the size of molecules, the slower the mobility becomes. Although discussing the effect of the size of thiolate is out of the scope of this study, a qualitative behavior does not come into conflict with the standard pattern of a series of AuSG clusters. We have also measured UV−vis absorption spectra of each fraction (Figure S3 in the Supporting Information). There is no sign of appearance of surface plasmon absorption for the isolated clusters from fraction **19** (core diameter 1.55 nm). The location of the first absorption peaks is plotted as a function of the number of gold atoms in Figure 6. There is no abrupt change on this plot. The variation found in the plot of Figure 4 should correlate with conformational or compositional changes in the adsorbed thiolate layer and not with that of gold core (if so, this may reflect to absorption spectrum). Within the range of linear line, it is possible to estimate the number of ligands adsorbed on the gold core if we check the core size by an appropriate measurement and the mobility value using AuSG as a size marker molecule.

Conclusions

In summary, we have observed that the chemical composition of AuSG clusters could be roughly expressed by a power function of size of cluster. The mobility of the PAGE fraction is not a smooth function of the logarithm of the number of gold atoms but reveals two linear crossing lines, which are better fitted by logarithm of the number of thiolate molecules.

Acknowledgment. This work was supported in part by a Grant-in-Aid for Scientific Research (S: 16101003) from MEXT.

Supporting Information Available: Methodology of electrospray ionization mass spectrometry (ESI). TEM photographs and size histograms of fractions **9**, **13**, **15**, **17**, **19**, and **23**. Absorption spectra of fractions **9**−**19**. This material is available free of charge via the Internet at http://pubs.acs.org.

References and Notes

(1) (a) Hames, B. D.; Rickwood, D. *Gel Electrophoresis of Proteins. A Practical Approach*, 2nd ed.; IRL Press:1990. (b) Hames, B. D.; Rickwood, D. *Gel Electrophoresis of DNA. A Practical Approach*, 2nd ed.; IRL Press: 1990.

(2) (a) Morris, C. J. O. R.; Morris, P. *Biochem. J.* **1971**, *124*, 517. (b) Weber, K.; Osborn, M. *J. Biol. Chem.* **1969**, *244*, 4406. (c) Kashino, Y.; Koike, H.; Satoh, K. *Electrophoresis* **2001**, *22*, 1004.

(3) Arnaud, I.; Abid, J.-P.; Roussel, C.; Girault, H. H. *Chem. Commun.* **2005**, 787.

(4) Parak, W. J.; Pellegrino, T.; Micheel, C. M.; Gerion, D.; Williams, S. S.; Alivisatos, A. P. *Nano Lett.* **2003**, *3*, 33.

(5) (a) Lamber, R.; Wetjen, S.; Schulz-Ekloff, G. *J. Phys. Chem.* **1995**, *99*, 13834. (b) Harfenist, S. A.; Wang, Z. L.; Alvarez, M. M.; Vezmar, I.; Whetten, R. L. *J. Phys. Chem.* **1996**, *100*, 13904. (c) Brown, L. O.; Hutchison, J. E. *J. Am. Chem. Soc.* **1997**, *119*, 12384. (d) Wang, Z. L. *Adv. Mater.* **1998**, *10*, 13. (e) Kiely, C. J.; Fink, J.; Brust, M.; Bethell, D.; Schiffrin, D. J. *Nature* **1998**, *396*, 444. (f) Martin, J. E.; Wilcoxon, J. P.; Odinek, J.; Provencio, P. *J. Phys. Chem. B* **2000**, *104*, 9475. (g) Brown, L. O.; Hutchison, J. E. *J. Phys. Chem. B* **2001**, *105*, 8911. (h) Thomas, P. J.; Kulkarni, G. U.; Rao, C. N. R. *J. Phys. Chem. B* **2001**, *105*, 2515. (i) Stoeva, S. I.; Prasad, B. L. V.; Uma, S.; Stoimenov, P. K.; Zaikovski, V.; Sorensen, C. M.; Klabunde, K. J. *J. Phys. Chem. B* **2003**, *107*, 7441. (j) Sloufova-Smova, I.; Vlckova, B. *Nano Lett.* **2002**, *2*, 121. (k) Prasad, B. L. V.; Stoeva, S. I.; Sorensen, C. M.; Klabunde, K. J. *Langmuir* **2002**, *18*, 7515. (l) Kim, Y.-.G.; Oh, S.-.K.; Crooks, R. M. *Chem. Mater.* **2004**, *16*, 167. (m) Sato, S.; Wang, S.; Kimura, K. *J. Phys. Chem. C* **2007**, *111*, 13367.

(6) (a) Leopaold, D. G.; Ho, J.; Lineberger, W. C. *J. Chem. Phys.* **1987**, *86*, 1715. (b) Taylor, K. J.; Pettiette-Hall, C. L.; Cheshnovsky, O.; Smalley, R. E. *J. Chem. Phys.* **1992**, *96*, 3319. (c) Kim, H. K.; Wood, T. D.; Marshall, A. G.; Lee, J. *Chem. Phys. Lett.* **1994**, *224*, 589. (d) Whetten, R. L.; Khoury, J. T.; Alvarez, M. M.; Murthy, S.; Vezmar, I.; Wang, Z. L.; Stephens, P. W.; Cleveland, C. L.; Luedtke, W. D.; Landman, U. *Adv. Mater.* **1996**, *8*, 428. (e) Schaaff, T. G.; Shafigullin, M. N.; Khoury, J. T.; Vezmar, I.; Whetten, R. L.; Cullen, W. G.; First, P. N. *J. Phys. Chem. B* **1997**, *101*, 7885. (f) Arnold, R. J.; Reilly, J. P. *J. Am. Chem. Soc.* **1998**, *120*, 1528. (g) Negishi, Y.; Tsukuda, T. *J. Am. Chem. Soc.* **2003**, *125*, 4046.

(7) Yao, H.; Miki, K.; Nishida, N.; Sasaki, A.; Kimura, K. *J. Am. Chem. Soc.* **2005**, *127*, 15536.

(8) Nishida, N.; Yao, H.; Kimura, K. *Langmuir* **2008**, *24*, 2759.

(9) Nishida, N.; Yao, H.; Ueda, T.; Sasaki, A.; Kimura, K. *Chem. Mater.* **2007**, *19*, 2831.

(10) Schaaff, T. G.; Knight, G.; Shafigullin, N. N.; Borkman, R. F.; Whetten, R. L. *J. Phys. Chem. B* **1998**, *102*, 10643.

(11) Schasff, T. G.; Whetten, R. L. *J. Phys. Chem. B* **2000**, *104*, 2630.

(12) Negishi, Y.; Takasugi, Y.; Sato, S.; Yao, H.; Kimura, K.; Tsukuda, T. *J. Am. Chem. Soc.* **2004**, *126*, 6518.

(13) Negishi, Y.; Takasugi, Y.; Sato, S.; Yao, H.; Kimura, K.; Tsukuda, T. *J. Phys. Chem. B* **2006**, *110*, 12218.

(14) Negishi, Y.; Nobusada, K.; Tsukuda, T. *J. Am. Chem. Soc.* **2005**, *127*, 5261.

(15) Chen, S.; Yao, H.; Kimura, K. *Langmuir* **2001**, *17*, 733.

(16) Heaven, M. W.; Dass, A.; White, P. S.; Holt, K. M.; Murray, R. W. *J. Am. Chem. Soc.* **2008**, *130*, 3754.

(17) Whetten, R. L.; Price, R. C. *Science* **2007**, *318*, 407.

(18) Jadzinsky, P. D.; Calero, G.; Ackerson, C. J.; Bushnell, D. A.; Kornberg, R. D. *Science* **2007**, *318*, 430.

(19) Jiang, D.; Tiago, J. L.; Luo, W.; Dai, S. *J. Am. Chem. Soc.* **2008**, *130*, 2777.

(20) Chen, S.; Kimura, K. *Langmuir* **1999**, *15*, 1075.

(21) Kimura, K.; Yao, H.; Sato, S. *Synth. React. Inorg., Met.-Org. Nano-Met. Chem.* **2006**, *36*, 237.

(22) Badia, A.; Singh, S.; Demers, L.; Cuccia, L.; Brown, G. R.; Lennox, R. B. *Chem.—Eur. J.* **1996**, *2*, 359.
(23) (a) Sellers, H.; Ulman, A.; Schnidman, Y.; Eilers, J. E. *J. Am. Chem. Soc.* **1993**, *115*, 9389. (b) Camillone, N.; Chidsey, C. E. D.; Liu, G.; Putvinski, T. M.; Scoles, G. *J. Chem. Phys.* **1991**, *94*, 8493.
(24) Stellwagen, E.; Lu, Y.; Stellwagen, N. C. *Biochemistry* **2003**, *42*, 11745.
(25) Scopes, R. K. *Protein Purification. Principles and Practice*, 2nd ed.; Springer-Verlag: New York, Heidelberg, Berlin, London, Paris, Tokyo, 1988.

JP808967P